

PRIMARY RESEARCH ARTICLE

High carbon losses from oxygen-limited soils challenge biogeochemical theory and model assumptions

Wenjuan Huang¹  | Kefeng Wang²  | Chenglong Ye^{1,3}  | William C. Hockaday⁴  |
Gangsheng Wang⁵  | Steven J. Hall¹ 

¹Department of Ecology, Evolution, and Organismal Biology, Iowa State University, Ames, Iowa, USA

²College of Life Science, Northwest University, Xi'an, China

³Ecosystem Ecology Lab, College of Resources and Environmental Sciences, Nanjing Agricultural University, Nanjing, China

⁴Department of Geosciences, Baylor University, Waco, Texas, USA

⁵Institute for Water-Carbon Cycles and Carbon Neutrality, and State Key Laboratory of Water Resources and Hydropower Engineering Sciences, Wuhan University, Wuhan, China

Correspondence

Gangsheng Wang, Institute for Water-Carbon Cycles and Carbon Neutrality, and State Key Laboratory of Water Resources and Hydropower Engineering Sciences, Wuhan University, Wuhan 430072 China. Email: wang.gangsheng@gmail.com

Steven J. Hall, Department of Ecology, Evolution, and Organismal Biology, Iowa State University, Ames, IA 50011, USA. Email: stevenjh@iastate.edu

Funding information

National Science Foundation, Division of Environmental Biology, Grant/Award Number: 1457805; National Natural Science Foundation of China, Grant/Award Number: 41901059; National Science Foundation, Grant/Award Number: 1331841

Abstract

Oxygen (O₂) limitation contributes to persistence of large carbon (C) stocks in saturated soils. However, many soils experience spatiotemporal O₂ fluctuations impacted by climate and land-use change, and O₂-mediated climate feedbacks from soil greenhouse gas emissions remain poorly constrained. Current theory and models posit that anoxia uniformly suppresses carbon (C) decomposition. Here we show that periodic anoxia may sustain or even stimulate decomposition over weeks to months in two disparate soils by increasing turnover and/or size of fast-cycling C pools relative to static oxic conditions, and by sustaining decomposition of reduced organic molecules. Cumulative C losses did not decrease consistently as cumulative O₂ exposure decreased. After >1 year, soils anoxic for 75% of the time had similar C losses as the oxic control but nearly threefold greater climate impact on a CO₂-equivalent basis (20-year timescale) due to high methane (CH₄) emission. A mechanistic model incorporating current theory closely reproduced oxic control results but systematically underestimated C losses under O₂ fluctuations. Using a model-experiment integration (ModEx) approach, we found that models were improved by varying microbial maintenance respiration and the fraction of CH₄ production in total C mineralization as a function of O₂ availability. Consistent with thermodynamic expectations, the calibrated models predicted lower microbial C-use efficiency with increasing anoxic duration in one soil; in the other soil, dynamic organo-mineral interactions implied by our empirical data but not represented in the model may have obscured this relationship. In both soils, the updated model was better able to capture transient spikes in C mineralization that occurred following anoxic–oxic transitions, where decomposition from the fluctuating-O₂ treatments greatly exceeded the control. Overall, our data-model comparison indicates that incorporating emergent biogeochemical properties of soil O₂ variability will be critical for effectively modeling C-climate feedbacks in humid ecosystems.

KEYWORDS

carbon decomposition, carbon stable isotope, iron redox, methane, microbial model, mineral-associated carbon, ModEx, oxygen fluctuation

Wenjuan Huang and Kefeng Wang should be considered joint first authors.

This is an open access article under the terms of the Creative Commons Attribution-NonCommercial License, which permits use, distribution and reproduction in any medium, provided the original work is properly cited and is not used for commercial purposes.

© 2021 The Authors. *Global Change Biology* published by John Wiley & Sons Ltd.

1 | INTRODUCTION

The decomposition of organic C in soils and sediments to CO₂ (and to a lesser extent, CH₄) ranks among the largest global C fluxes. It is mediated by microbially catalyzed redox reactions, of which aerobic (O₂ dependent) respiration is most favorable from a thermodynamic perspective (Conrad, 1996). The importance of O₂ deprivation as a mechanism of soil C persistence has been well studied in wetlands and sediments (Arndt et al., 2013; Freeman et al., 2001), and is also increasingly recognized in well-drained upland soils, which contain anoxic microsites (Keiluweit et al., 2016). However, soil O₂ availability may also be temporally dynamic (O'Connell et al., 2018). In contrast with current theory and models, C decomposition under temporal O₂ fluctuations may differ from rates observed under constant oxic or anoxic conditions (DeAngelis et al., 2010; Lin et al., 2021; Pett-Ridge & Firestone, 2005; Reddy & Patrick, 1975). Furthermore, the intensification of hydrological cycles as a consequence of climate change (IPCC, 2014) and land use change (Piao et al., 2007) will likely alter temporal patterns of soil O₂ availability. Anoxic events over timescales of days to weeks may increasingly occur in a warmer and wetter world due to increased biological O₂ demand, lower O₂ solubility, and larger precipitation events (Calabrese & Porporato, 2019; Griffis et al., 2017; Hall et al., 2013; Liptzin et al., 2011; Figure 1a). Oxygen fluctuations are especially important in hydric soils (Jarecke et al., 2016), which experience periodic saturation and are globally widespread: in the United States, soil map units with at least a partial hydric component conservatively account for >31% of total land area (Figure 1b). Thus, it is critical to better understand how soil O₂ fluctuations associated with hydrologic variability affect C losses as CO₂ and CH₄.

Traditional theory and mechanistic models postulate a monotonic decrease in C decomposition rate as O₂ availability decreases (e.g., Figure 1c), irrespective of temporal scale. Sustained O₂ limitation has been long known to decrease soil C decomposition (Greenwood, 1961) by inhibiting oxidative enzymes and decreasing microbial growth and metabolism relative to oxic conditions (Freeman et al., 2001; McLatchey & Reddy, 1998). The decomposition rates of both faster- and slower-cycling C pools are thought to decrease under O₂ limitation (Sierra et al., 2017; Figure 1c), commonly represented in ecosystem models using a constant scalar factor or Michaelis-Menten kinetics (Davidson et al., 2012; Koven et al., 2013; Oleson et al., 2013; Riley et al., 2011; Rubol et al., 2013). Anoxia also promotes methane (CH₄) production, which has 84 times the global warming potential of CO₂ over a 20-year timescale (Myhre et al., 2013). However, net CH₄ production from soils experiencing episodic anoxia over days to weeks is generally expected to be small, as methanogenesis is traditionally assumed to occur only after prolonged anoxic periods, when alternative electron acceptors such as iron (Fe) or sulfate have been consumed (Conrad, 1996; Reddy & Patrick, 1975; Riley et al., 2011).

These assumptions imply that periodic O₂ deprivation should decrease both total C losses and climate impact on a CO₂-equivalent basis (Figure 1c). However, recent experimental studies in soils subjected to sequential anoxic and oxic conditions challenge these ideas (Bhattacharyya et al., 2018; DeAngelis et al., 2010; Longhi et al., 2016). Thermodynamic constraints on C decomposition could be compensated by other biogeochemical processes that increase C availability under fluctuating O₂, such as Fe redox cycling and release of mineral-protected C (Chen et al., 2018, 2020; Huang & Hall, 2017b; Huang et al., 2020). Furthermore, even the intermittent presence of O₂ may sustain metabolism of reduced substrates (e.g., lipids) accumulated under anoxia (Burdige, 2007). Sustained and significant CH₄ production may occur even when O₂ is periodically present (Angle et al., 2017; Huang & Hall, 2018; Silver et al., 1999), challenging model assumptions (Riley et al., 2011). Rigorous model-data synthesis is needed to evaluate the possibility that periodic anoxia (i.e., O₂ fluctuations) characteristic of many hydric and even upland soil environments could lead to equal or greater CO₂-equivalent greenhouse gas emissions relative to static oxic conditions, counter to current prevailing theory (Figure 1c).

Current mechanistic models that incorporate microbial processes (known as "microbial models") are capable of closely representing laboratory- and field-scale decomposition data from terrestrial ecosystems in some cases (Bradford et al., 2016; Meile & Scheibe, 2018; Wang et al., 2015, 2019). Models increasingly incorporate O₂ availability as a control on biogeochemical process rates (Davidson et al., 2012; Koven et al., 2013; Oleson et al., 2013; Riley et al., 2011; Rubol et al., 2013), with parameters that were defined from short-term experiments comparing oxic and anoxic conditions (Sierra et al., 2017). Yet, we are unaware of explicit tests and validation of their underlying assumptions in environments where O₂ availability varies over time. In particular, parameters derived from short-term incubations (i.e., hours to several weeks) could bias model parameterization and predictions (Jian et al., 2020). Integration of long-term (months–years) incubation datasets with microbial models remains quite limited (Jian et al., 2020). Here we used a high-resolution experiment-model comparison with 2–4-day measurement timesteps and hourly model timesteps over a 384-day experiment to test theory and model assumptions about biogeochemical responses to frequent temporal changes in O₂ availability.

We examined the response of CO₂ and CH₄ production (C mineralization) to cyclic, time-varying O₂ fluctuations in two soils known to experience periodic anoxia: an Oxisol from a humid tropical forest and a Mollisol from a temperate agroecosystem. Litter from a C₄ grass (*Andropogon gerardii*) was added to both soils, and carbon isotope ratios (δ¹³C) of CO₂ and CH₄ were measured to partition decomposition between litter and soil sources. Soils were incubated under a static oxic control and four fluctuating-O₂ treatments for 384 days. The fluctuating-O₂ treatments consisted of either 2, 4, 8, or 12 days of anoxic conditions followed by 4 days of oxic conditions, cycles which were repeated

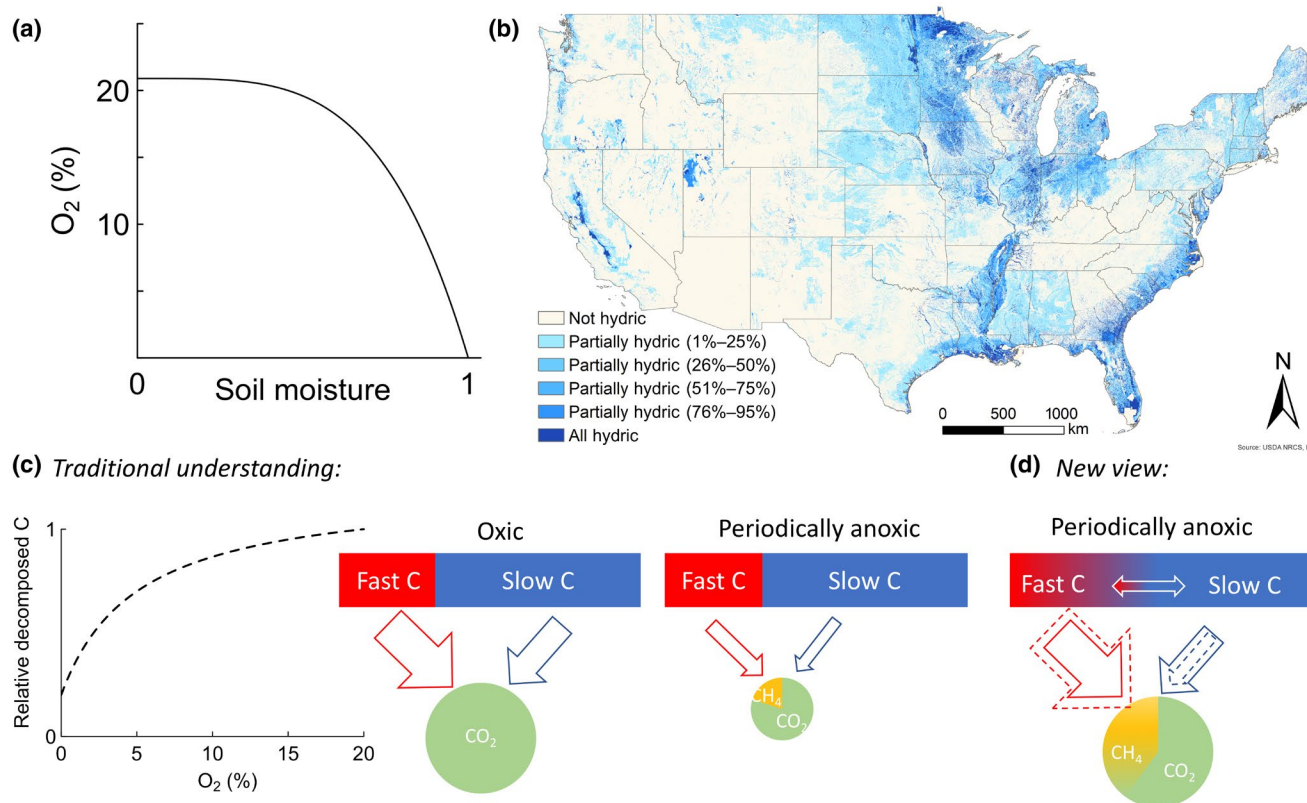


FIGURE 1 Conceptual frameworks for soil C decomposition response to soil O_2 fluctuations associated with hydrological cycles under climate change. (a) A typical relationship between soil pore O_2 concentration and moisture (Calabrese & Porporato, 2019; Hall et al., 2013). (b) Distribution of hydric soils in the contiguous United States (Soil Survey Staff, Natural Resources Conservation Service, United States Department of Agriculture, 2019). (c) Conceptual views for the responses of soil C decomposition to static oxic and periodically anoxic conditions, with relative pool sizes and fluxes indicated by boxes and arrow widths. The traditional understanding is that C decomposition rate declines as O_2 availability decreases and that O_2 fluctuations over days–weeks (periodic anoxia) consistently suppress the decomposition of fast and slow C pools, with minor CH_4 emissions. (d) The new view proposed here is that O_2 fluctuations alter the pools sizes and/or fluxes of fast and slow C pools decomposed to CO_2 and CH_4 and increase global warming potential due to sustained CH_4 emission. The gradient colors indicate that the sizes of C pools change as a function of anoxic durations. The arrows with both dotted and solid lines indicate that the decomposition rates of C pools change as a function of anoxic durations

for the duration of the experiment. These treatments are hereafter denoted by the length of their anoxic phases (2-, 4-, 8-, and 12-day treatments; Figure S1). The periodicity of O_2 fluctuations employed here mimicked patterns observed in the field, where recurring anoxic events may occur over days–weeks in response to precipitation dynamics (Liptzin et al., 2011; Logsdon, 2015). The incubation experiment was used to test the conventional understanding of how O_2 limitation impacts C decomposition under current model assumptions, whereby decomposition decreases monotonically with increasing anoxic duration. The Microbial-ENzyme Decomposition (MEND) model (Wang et al., 2019) with a new CH_4 module was used to simulate C mineralization responses to fluctuating O_2 (Figure S2). We first parameterized the MEND model using data from the control only and employed it under the current assumptions of the model to test the consensus understanding of how O_2 limitation impacts C decomposition. We then parameterized the MEND model using data from all treatments to estimate key model parameters representing biogeochemical processes that may compensate for O_2 limitation on decomposition.

2 | MATERIALS AND METHODS

2.1 | Soil sampling

An Oxisol and Mollisol, which are both characterized by redox fluctuations under field conditions, were sampled in March 2017 in a perhumid tropical forest near the El Verde field station of the Luquillo Experimental Forest (18°17'N, 65°47'W), Puerto Rico and an agricultural field in north-central Iowa (41°75'N, 93°41'W), USA, respectively. The Oxisol was from an upland valley in the Bisley watershed, with mean annual precipitation and temperature of 3800 mm and 24°C, respectively. Soil was formed from volcanoclastic sediment (Buss et al., 2017). The Oxisol experiences O_2 fluctuations on scales of hours to weeks due to variations in rainfall and biological O_2 demand (Liptzin et al., 2011). Soil was randomly sampled from the A horizon (0–10 cm) by compositing six replicate soil cores without disturbing microaggregate structure (no sieving), and then shipped overnight to Iowa State University. The Mollisol was sampled from a topographic

depression that experiences periodic flooding (Logsdon, 2015) in the Walnut Creek watershed, with mean annual precipitation of 820 mm and mean monthly temperature ranging from -13.4°C (January) to 29.4°C (July; Hatfield et al., 1999). This very poorly drained soil was formed from till following the Wisconsin glaciation and developed under tallgrass prairie and wetland vegetation, and is described as mucky silt loam (fine, montmorillonitic, mesic Cumulic Haplaquoll). This site was cultivated with corn (*Zea mays*) and soybean (*Glycine max*) rotated on an annual basis. We collected soils from the plow layer A horizon (0–20 cm) following corn cultivation. Six soil cores (10.2 cm diameter) were randomly sampled in a $50 \times 50\text{-m}$ region and then composited.

2.2 | Laboratory incubations

We amended soils with finely ground leaf tissue of *Andropogon gerardii* (big bluestem, a C_4 grass), which ameliorated short-term C limitation of microbial metabolism (Chacon et al., 2006) and provided an isotopic contrast with extant C. Soils were gently mixed after coarse roots, organic debris and macrofauna (worms) were manually removed. Field moisture capacity was determined by saturating soils and then measuring gravimetric water content following 48 h of drainage ($1.01 \text{ g H}_2\text{O g}^{-1}$ soil for the Oxisol and $0.46 \text{ g H}_2\text{O g}^{-1}$ soil for the Mollisol). Aliquots of litter (500 mg) were gently homogenized with fresh soil subsamples (5 g dry mass equivalent), and deionized water was added to achieve field moisture capacity. Each replicate was incubated in an open 50 ml centrifuge tube placed in a glass jar (946 ml) and sealed with a gas-tight aluminum lid with butyl septa for headspace gas purging and sampling.

Replicates from each soil were incubated under five headspace treatments in the dark at 23°C for 384 days, including a static oxic control and four fluctuating- O_2 treatments. Carbon mineralization data from the static oxic controls were previously published in a companion experiment that compared the impacts of long-term oxic versus anoxic conditions on soil C cycling (Huang et al., 2020). The fluctuating- O_2 treatments consisted of either 2, 4, 8, or 12 days of anoxic conditions followed by 4 days of oxic conditions, cycles which were repeated for the duration of the experiment. The fluctuating- O_2 treatments are denoted by the length of the anoxic phase (2-, 4-, 8-, and 12-day treatments, respectively). There were five replicates for each headspace treatment (total $n = 50$). To achieve anoxic and oxic phases according to the above treatments, each jar was flushed with humidified N_2 or CO_2 -free air, respectively, at 500 ml min^{-1} for 15 min immediately following headspace sampling for CO_2 and CH_4 measurements. Sample masses were recorded and additional water was added as necessary at approximately 8-day intervals to replace moisture loss during headspace flushing.

2.3 | Analysis of CO_2 and CH_4 production

Gas samples (5 ml) were collected immediately prior to headspace flushing for measurements of CO_2 concentration and $\delta^{13}\text{C}$

values using a tunable diode laser absorption spectrometer (TDLAS, TGA200A, Campbell Scientific; Hall et al., 2017). Measurements were conducted daily for the first month and every 2 days thereafter in the control and fluctuating- O_2 treatments. Additional gas samples (20 ml) were collected at 4-day intervals to measure CH_4 concentration by gas chromatography (GC) with a flame ionization detector (GC-2014, Shimadzu). CH_4 production over 2-day intervals was estimated from the average of consecutive 4-day measurements (for the 2-day treatment, 4-day averages were calculated between adjacent measurements with the same sequence of anoxic/oxic phase transition). We also measured $\delta^{13}\text{C}$ values of CH_4 by TDLAS every 4 days in order to achieve C isotope mass balance and account for the effects of CH_4 production on the $\delta^{13}\text{C}$ values of CO_2 due to methanogenesis and methane oxidation (Huang & Hall, 2018; Whiticar, 1999). We chemically removed CO_2 from each gas sample and then combusted CH_4 to CO_2 (Huang & Hall, 2018). For the 4-, 8- and 12-day treatments, the $\delta^{13}\text{C}$ values of CH_4 were measured at 2-day intervals prior to 84 days and subsequently at 4-day intervals. The $\delta^{13}\text{C}$ values of CH_4 were interpolated over 2-day intervals using the same method for CH_4 production estimates. The CO_2 -equivalent greenhouse gas emission was calculated over a 20-year timescale by multiplying CH_4 mass by 84 (1 g $\text{CH}_4 = 84 \text{ g}$ of CO_2 equivalent) and adding to the CO_2 mass (Myhre et al., 2013). Net N_2O production was negligible in our experiment, determined by periodic measurements of N_2O by gas chromatography concomitant with CH_4 measurements.

Total C mineralization from litter and soil in the Oxisol and Mollisol at the end of experiment was calculated by multiplying cumulative mineralized C by its respective fractional contributions, which were determined by two-source mixing models described in the Supplementary Methods. The fractions of total C mass remaining in the Oxisol and Mollisol over time were calculated by subtracting cumulative total C mineralization from initial C (415 and 386 mg C for the Oxisol and Mollisol, respectively).

2.4 | Soil chemical analyses

We measured net Fe reduction and dissolved organic carbon (DOC) released by water extractions in additional replicate samples from each soil and headspace treatment during the initial 48 days. Three replicates per treatment were destructively sampled every 4 days for the control and at the end of each anoxic/oxic phase for the fluctuating- O_2 treatments. Soil subsamples were extracted in 0.5 M hydrochloric acid (HCl) for net Fe reduction and nanopure water for DOC in a 1:60 dry soil-to-solution ratio. Iron concentrations in 0.5 M HCl extractions (denoted $\text{Fe(II)}_{\text{HCl}}$ and $\text{Fe(III)}_{\text{HCl}}$) were determined colorimetrically by ferrozine (Huang & Hall, 2017a). The DOC concentrations were measured on a Shimadzu TOC-L analyzer.

At the end of this experiment (384 days), soil subsamples were analyzed for dissolved organic C (DOC) concentrations in water ($\text{DOC}_{\text{H}_2\text{O}}$) and several sequential extractions. The first extraction was sodium sulfate ($\text{DOC}_{\text{Na}_2\text{SO}_4}$), which releases C from weak

polyvalent cation bridges (Ye et al., 2018), followed by sodium dithionite ($\text{DOC}_{\text{Na}_2\text{S}_2\text{O}_4}$), which releases C sorbed or co-precipitated with reducible Fe phases (Wagai & Mayer, 2007), and finally sodium pyrophosphate ($\text{DOC}_{\text{Na}_4\text{P}_2\text{O}_7}$), which releases C in organo-metal/mineral complexes (Coward et al., 2017). The $\text{DOC}_{\text{Na}_2\text{SO}_4}$ values were corrected for $\text{DOC}_{\text{H}_2\text{O}}$ measured on separate soil subsamples ($n = 5$) extracted by nanopure water in a 1:60 dry soil-to-solution ratio. For the additional sequential extractions, subsamples were first extracted by 0.5 M Na_2SO_4 at a soil-to-solution ratio (g ml^{-1}) of 0.0056 for 1 h, followed by 0.266 g $\text{Na}_2\text{S}_2\text{O}_4$ (0.05 M) and 30 ml deionized water for 16 h. Then, to dissolve any sulfide-associated elements, soils were extracted in 0.05 M HCl for 1 h, prior to extraction with 0.1 M $\text{Na}_4\text{P}_2\text{O}_7$ for 16 h (Huang et al., 2019). Following each extraction, slurries were centrifuged at 20,000 g for 10 min and supernatant solutions were stored at 4°C prior to analysis. The DOC concentrations and their $\delta^{13}\text{C}$ values were analyzed by measuring CO_2 and $\delta^{13}\text{C}$ produced from sample oxidation by boiling with persulfate in serum vials followed by injection of the headspace gas on TDLAS (Huang & Hall, 2017b). The soluble litter- and soil-derived C in each extraction was estimated as the product of DOC concentration and the respective fractional contributions from litter and soil calculated using the isotope mixing models described above.

Two replicate soil subsamples from each treatment after the 384-day incubation were analyzed by ^{13}C nuclear magnetic resonance (NMR) spectroscopy to assess organic C molecular composition. More details on the ^{13}C NMR analysis are provided in Supplementary Methods.

2.5 | Data analysis

A mixed-effects model was used to test differences among treatments (fixed effects) in each soil for instantaneous CO_2 and CH_4 production, using the “lmer” function in R (Bates et al., 2015). Samples were treated as random effects to account for repeated sampling. Dunnett’s test was used to compare the variables in the fluctuating- O_2 treatments with the static oxic control for each soil. Relationships between soil properties and anoxic phase duration were analyzed by linear regression models using the “lm” function in R. We also performed linear regression to analyze the response of cumulative C decomposition to relative O_2 concentration and variance. The O_2 availability was treated as a discrete random variable in our study. Thus, the O_2 variance was determined by summing the product of the probability of anoxic or oxic phases occurring in one cycle of each fluctuating- O_2 treatment, and the square of the difference between relative O_2 concentrations (0 for anoxic and 1 for oxic phases) and the weighted relative O_2 concentrations by their probability. The O_2 variance was then normalized by the sum of O_2 variances in all fluctuating- O_2 treatments to calculate the relative O_2 variance. We modeled trends in the fractions of C mass remaining over time using two-pool first-order exponential decay models using the “nls” function in R. Likelihood ratio tests comparing nested models were used to assess whether decomposition rate constants differed among

treatments. The parameters from the two-pool first order exponential decay models were also used to simulate instantaneous total C decomposition rate ($\text{CO}_2 + \text{CH}_4$, defined hereafter as C mineralization) and to evaluate model performance by calculating the Akaike information criterion (AIC) (see below) to compare with the MEND model performance.

2.6 | Process-based model simulation

The MEND model (Wang et al., 2013, 2015, 2019) explicitly represents: (i) density-based partitioning and physicochemical protection of soil organic matter (SOM); (ii) distinct microbial and enzyme functional groups regulating SOM decomposition; and (iii) microbial physiology such as growth and maintenance, dormancy, resuscitation, and mortality in response to changes in soil pH, temperature, moisture, and oxygen availability. In this study, we incorporated a CH_4 module (Zhu et al., 2014) to simulate CH_4 production and oxidation (Figure S2). Governing equations of soil C pools (Figure S2; Table S2) in the MEND model are shown in Table S3. Component fluxes and parameters in the MEND model are described in Tables S4 and S5.

The modified MEND model used O_2 scalars to represent the impacts of O_2 availability on multiple aspects of soil C processes (Tables S3 and S4). Values of these scalars were determined by comparing data from the static oxic control and the static anoxic treatment in a companion experiment with these same soils described in Huang et al. (2020). The MEND model simulated reversible dynamic transformations between two microbial functional groups (i.e., active and dormant microbes), where only the active microbes could take up C and nutrients and reproduce. In addition to the dependence of microbial dormancy on substrate and soil moisture availability, we assumed that more microorganisms were active under oxic than anoxic conditions (Eq. S38). In addition, CH_4 production flux was a fraction of total C mineralization flux (Eq. S28), where the fraction (r_{CH_4}) is modified by soil pH, temperature, and O_2 availability. The actual CH_4 production fraction (i.e., r_{CH_4} modified by environmental factors) represented the methanogenic activity compared to the total microbial activity mediating C mineralization. The CH_4 oxidation flux was simulated as a fraction of CH_4 production flux (Eq. S29), where the fraction (i.e., the CH_4 oxidation coefficient f_{CH_4}) followed Michaelis–Menten kinetics and was modified by soil temperature and O_2 availability. With increasing O_2 availability, CH_4 production rate decreased and oxidation rate increased (Eq. S39). Initial C pool values are provided in the Supplementary Methods. The MEND model runs at an hourly timestep.

We applied the multi-objective calibration method to determine selected MEND model parameters (Duan et al., 1992; Wang et al., 2015). Six calibrated parameters included CH_4 production as a fraction (r_{CH_4}) of total active microbial respiration, two parameters controlling microbial growth and maintenance (V_g and V_m), and three parameters regulating enzyme production and turnover (p_{EP} , fp_{EM} , and r_E ; see Table S5 for further description). Here, microbial maintenance (V_m , mg C mg^{-1} active-biomass- C h^{-1}) refers to additional consumption

of energy and C for purposes other than biomass production (Wang & Post, 2012). The other model parameters were fixed based on previous studies (Wang et al., 2013, 2015, 2019). Each objective evaluated goodness-of-fit of a specific observed variable, for example, daily CO₂ and CH₄ fluxes. Parameter optimization minimized the total objective function (J) computed as the weighted average of multiple objectives. The individual objective function J_i (i.e., for CO₂ and CH₄ fluxes) was calculated as $(1 - R^2)$, where R^2 denoted the coefficient of determination and a higher R^2 indicates better model fitness (Wang et al., 2019). We used the shuffled complex evolution (SCE) algorithm (Duan et al., 1992; Wang et al., 2015) to search the optimal model parameters that minimize J . In addition, we used the AIC, corrected AIC (AICc), and Bayesian information criterion (BIC) to evaluate effects of different parameters (Johnson & Omland, 2004), that is, all six parameters, three parameters (r_{CH_4} , α , and fp_{EM}), and two parameters (r_{CH_4} and α). These criteria (AIC, AICc, and BIC) consider both model fit (i.e., the mean squared error) and complexity (i.e., the number of free parameters and the number of observations). The smaller the criterion value, the better the simulation (Johnson & Omland, 2004).

In our study, mean CO₂ flux was one order of magnitude higher than mean CH₄ flux under the control treatment. To make selection criteria comparable between different variables, we normalized the sum of squares of residuals (SSR) by the total sum of squares (SST) in the calculation of the likelihood (Johnson & Omland, 2004). Given that $\text{SSR}/\text{SST} = 1 - R^2$ (R^2 denotes the coefficient of determination; Wang et al., 2015), we modified the three criteria as follows:

$$\text{AIC} = n \cdot \ln\left(\frac{1 - R^2}{n}\right) + 2p,$$

$$\text{AIC}_c = n \cdot \ln\left(\frac{1 - R^2}{n}\right) + 2p \cdot \left(\frac{n}{n - p - 1}\right),$$

$$\text{BIC} = n \cdot \ln\left(\frac{1 - R^2}{n}\right) + p \cdot \ln(n),$$

where AIC, AIC_c, and BIC are defined above; $\ln(\cdot)$ denotes the natural logarithm; R^2 is coefficient of determination between simulated values ($y_{\text{sim}}(i)$) and observed values ($y_{\text{obs}}(i)$); n denotes the number of observations (i.e., sample size); and p denotes the number of free parameters.

3 | RESULTS

3.1 | Observed C mineralization

We found that the overall impact of fluctuating O₂ availability on C mineralization was generally similar in both the Oxisol and Mollisol and challenged prevailing assumptions of how O₂ limitation impacts decomposition. The treatments with increasingly longer anoxic phases depressed CO₂ production to a greater degree during periods of anoxia. However, CO₂ production in the subsequent oxic phases rebounded to a greater degree in treatments with longer anoxic duration (Figure 2a,b),

and largely (if not completely) compensated for decreased anoxic decomposition over most of the experiment. Total C mineralization from the fluctuating-O₂ treatments varied over time due to the changing magnitude of the decomposition pulse following each anoxic-oxic transition. Over the first few days-weeks of the experiment, treatments with longer anoxic duration tended to suppress total C loss, but this was invariably followed by a period of stimulated decomposition. This is demonstrated by expressing C mineralization from the fluctuating-O₂ treatments as a ratio relative to the control: ratios >1 were observed from the first week up to 9 months, depending on the particular soil and treatment (Figure 2e-h). In general, relative C mineralization ratios >1 occurred later in treatments with longer anoxic duration (Figure 2g,h). Eventually, C mineralization from all of the fluctuating-O₂ treatments decreased relative to the control. However, by the end of experiment, cumulative C mineralization from the Oxisol was statistically equivalent among the control ($274 \pm 23 \text{ mg g}^{-1} \text{ C}$) and the 12-day ($254 \pm 6 \text{ mg g}^{-1} \text{ C}$), 8-day ($237 \pm 9 \text{ mg g}^{-1} \text{ C}$), and 4-day ($234 \pm 4 \text{ mg g}^{-1} \text{ C}$) treatments, and was only significantly lower in the 2-day treatment ($227 \pm 9 \text{ mg g}^{-1} \text{ C}$; $p < .05$). Cumulative C mineralization from the Mollisol was similar between the control ($258 \pm 9 \text{ mg g}^{-1} \text{ C}$) and the 12-day treatment ($238 \pm 2 \text{ mg g}^{-1} \text{ C}$), whereas the 8-day ($234 \pm 6 \text{ mg g}^{-1} \text{ C}$; $p < .05$), 4-day ($233 \pm 3 \text{ mg g}^{-1} \text{ C}$; $p < .05$), and 2-day ($222 \pm 5 \text{ mg g}^{-1} \text{ C}$; $p < .01$) treatments were slightly but significantly lower than the control.

Despite the general similarities in CO₂ production among treatments, the CO₂-equivalent greenhouse gas emissions over a 20-year timescale significantly increased with anoxic phase duration in both soils due to CH₄ production ($p < .01$; Figure 3), which increased with anoxic phase duration and continued during the oxic treatment phases (Figure 2c,d). Overall, the contribution of CH₄ emission to total mineralized C increased with anoxic duration (from $3.3 \pm 0.9\%$ in the 2-day treatment to $12.4 \pm 1.7\%$ in the 12-day treatment for the Oxisol and from $1.5 \pm 0.6\%$ to $7.8 \pm 0.9\%$ for the Mollisol), and was negligible in the control ($0.3 \pm 0.1\%$ for the Oxisol and $0.5 \pm 0.2\%$ for the Mollisol). Correspondingly, the CO₂-equivalent greenhouse gas emissions in the 12-day treatment rose to 437% of the control in the Oxisol and 292% of the control in the Mollisol.

3.2 | Sources of decomposed C

Differences in $\delta^{13}\text{C}$ values of total mineralized C (CO₂ + CH₄) among treatments (Figure S3) showed that soil- and litter-derived C responded differently to the fluctuating-O₂ treatments. The $\delta^{13}\text{C}$ values of total mineralized C tended to decrease during oxic phases relative to anoxic phases, indicating that soil-derived C drove the increased C mineralization that typically occurred at the beginning of each oxic phase (Figure 2a,b). The difference in cumulative $\delta^{13}\text{C}$ values of total mineralized C at the end of experiment showed that the fluctuating-O₂ treatments generally suppressed losses of litter-derived C, but not soil-derived C, relative to the control (Figures S3 and S4). We also found that DOC_{H₂O} increased under the anoxic versus oxic phases and increased with anoxic phase duration during the first 48 days (Figure S5a,b). At the end of experiment, the fluctuating-O₂ treatments had

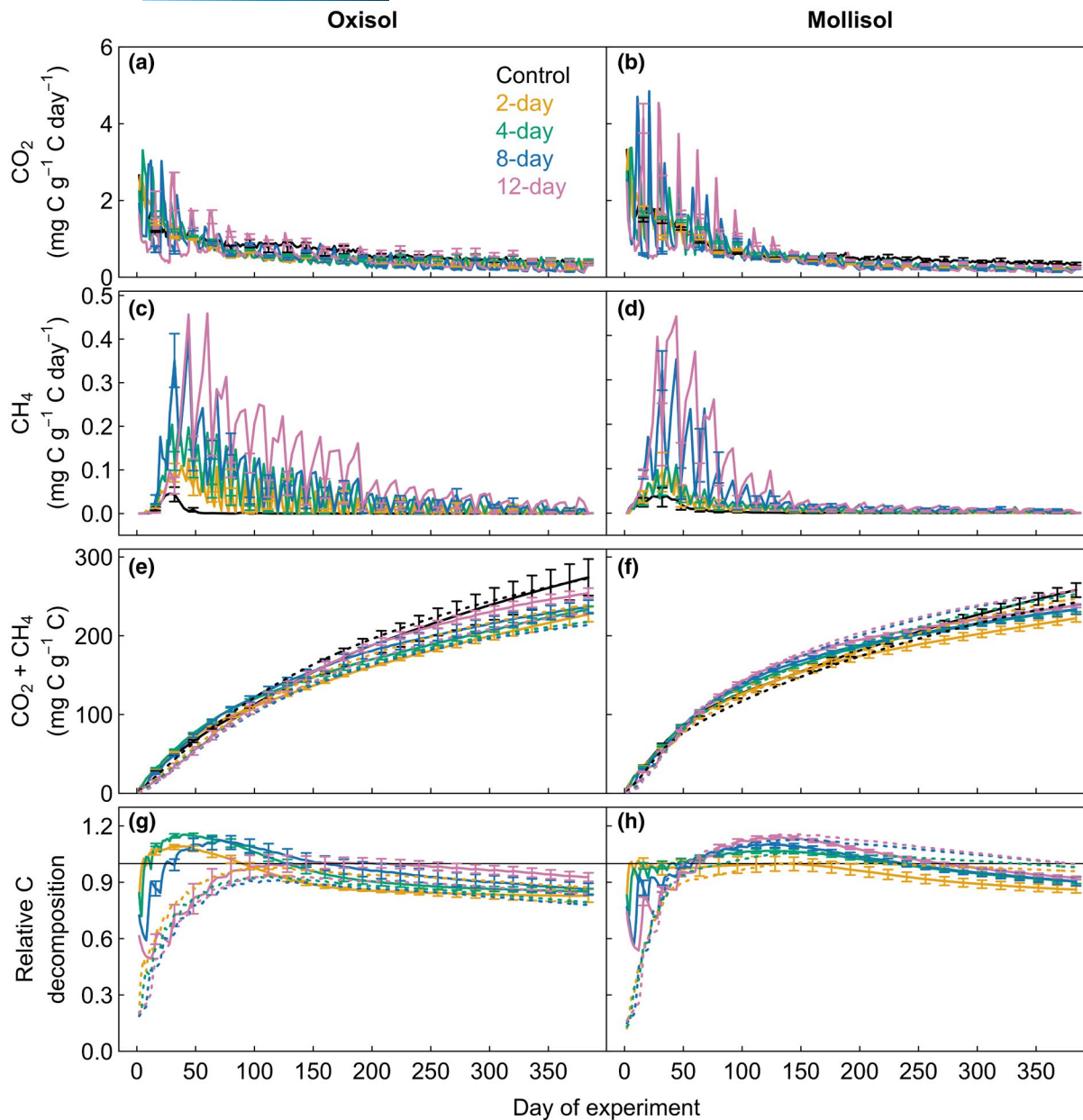


FIGURE 2 Measured (solid lines) and modeled (dotted lines) C decomposition from the Oxisol and Mollisol incubated under the static oxalic control and fluctuating-O₂ treatments. The 2-, 4-, 8-, and 12-day treatments indicate the fluctuating-O₂ treatments, which consisted of repeated cycles of 2, 4, 8, or 12 days of anoxia followed by 4 days of oxic conditions, respectively. Insets are expanded views of CO₂ and CH₄ production over the first 48 days. Measured CO₂ production in the Oxisol (a) and Mollisol (b); measured CH₄ production in the Oxisol (c) and Mollisol (d); measured and modeled cumulative total C decomposition in the Oxisol (e) and Mollisol (f); measured and modeled total C decomposition normalized by the value in the control in the Oxisol (g) and Mollisol (h). The solid lines represent the observations, and the dotted lines represent simulations by MEND model calibrated with the full dataset. The error bars plotted every 16 days for the observations indicate SEM ($n = 5$)

greater net losses of mineral-associated soil C relative to the control in the Oxisol, measured by sequential chemical extractions (Figure S6). For the Mollisol, there were some greater net losses of litter-derived DOC_{H₂O} and mineral-associated litter C (DOC_{Na₂SO₄} + DOC_{Na₄P₂O₇}) under the fluctuating-O₂ treatments relative to the control (Figure S6). However, we did not observe any differences in C chemical composition or oxidation state among treatments, as indicated by solid-state ¹³C NMR (Table S1).

Next, to examine the time-integrated responses of faster- and slower-cycling C pools to the fluctuating-O₂ treatments, we fit simple statistical models (two-pool, first-order decay) to the cumulative C mass remaining over time (Figure S7). We emphasize that the pool sizes and decomposition rate constants estimated by this approach are strictly empirical, represent long-term mean treatment responses, and cannot simulate instantaneous changes in decomposition following oxalic/anoxic transitions. The models fit the data very well,

FIGURE 3 CO₂-equivalent greenhouse gas emissions (20-year timescale) under the static oxalic control and fluctuating-O₂ treatments. The value was expressed relative to the initial dry mass of the soil + litter. The 2-, 4-, 8-, and 12-day treatments indicate the fluctuating-O₂ treatments, which consisted of repeated cycles of 2, 4, 8, or 12 days of anoxia followed by 4 days of oxalic conditions, respectively. The * and ** indicate significant differences between a treatment and the control at $p < .05$ and $.01$, respectively. The error bars indicate SEM ($n = 5$)

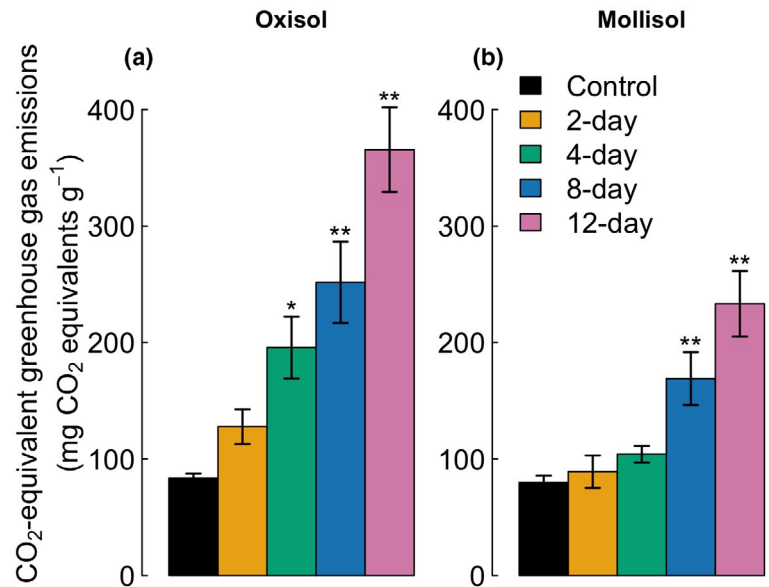


TABLE 1 Parameters for two-pool first-order decay models fit to the fractions of total C mass remaining in the Oxisol and Mollisol incubated under the static oxalic control and fluctuating-O₂ treatments. The 2-, 4-, 8-, and 12-day treatments indicate the fluctuating-O₂ treatments, which consisted of repeated cycles of 2, 4, 8, or 12 days of anoxia followed by 4 days of oxalic conditions, respectively

Treatment	f_f	k_f (year ⁻¹)	T_f (year)	f_s	k_s (year ⁻¹)	T_s (year)	R^2	T (year)
Oxisol								
Control	0.10 ± 0.00	3.86 ± 0.15	0.26	0.90	0.21 ± 0.00	4.8	0.9992	4.3
2 days	0.08 ± 0.00**	7.77 ± 0.10**	0.13	0.92	0.17 ± 0.00**	5.9	0.9997	5.4
4 days	0.10 ± 0.00	6.67 ± 0.03**	0.15	0.90	0.16 ± 0.00**	6.4	0.9999	5.8
8 days	0.16 ± 0.00**	3.71 ± 0.04	0.27	0.84	0.10 ± 0.00**	10.0	0.9998	8.5
12 days	0.32 ± 0.04**	1.59 ± 0.14**	0.63	0.68	0.00 ± 0.03**		0.9981	
Mollisol								
Control	0.09 ± 0.00	8.71 ± 0.11	0.11	0.91	0.20 ± 0.00	5.0	0.9996	4.6
2 days	0.13 ± 0.00**	5.94 ± 0.05**	0.17	0.87	0.11 ± 0.00**	8.9	0.9998	7.8
4 days	0.15 ± 0.00**	5.08 ± 0.04**	0.20	0.85	0.10 ± 0.00**	9.9	0.9998	8.4
8 days	0.17 ± 0.00**	4.36 ± 0.07**	0.23	0.83	0.08 ± 0.00**	13.2	0.9991	11.0
12 days	0.22 ± 0.01**	3.35 ± 0.11**	0.30	0.78	0.03 ± 0.01**	37.0	0.9973	28.9

Note: Values are means and SEM; f_f and f_s , fractions of C in the fast and slow pools; k_f and k_s , decomposition rates of the fast and slow C pools; T_f , T_s , and T , turnover rates of the fast, slow, and total C pools.

**Denotes $p < .01$.

with R^2 values of .9973–.9999; rate constants indicated mean turnover times of months and years for fast and slow pools, respectively (Table 1; Figure S7). In both soils, decreasing cumulative O₂ availability increased mean turnover times of total C, calculated as the mass-weighted average of both pools. However, in the Oxisol, the 2- and 4-day treatments significantly increased the decomposition rate of the fast C pool relative to the control ($p < .01$ for all), whereas the 8- and 12-day treatments significantly increased the proportion of C in the fast pool. In the Mollisol, the proportion of C in the fast pool significantly increased in the fluctuating-O₂ treatments ($p < .01$ for all), although its decomposition rate decreased. Next, we asked what mechanism(s) contributed to the observed changes in C mineralization under the fluctuating-O₂ treatments.

3.3 | Integrating experimental data with a mechanistic model (MEND)

To test our existing understanding of how O₂ limitation alters decomposition, we first simulated the impacts of fluctuating O₂ availability under the current assumptions of our mechanistic model (MEND), which are shared by other models. That is, we used data from the oxalic control for model parameterization and applied a scalar to suppress decomposition under anoxic conditions, where the scalar was calibrated by the data from a static anoxic incubation in a companion study (Huang et al., 2020). In the control, the model closely reproduced observed trends in C mineralization over time (Figures S8a,b and S9a,b). However, in the fluctuating-O₂ treatments, the model generally failed to capture the temporal pulses

of C mineralization during anoxic/oxic transitions—mostly underestimating, but occasionally overestimating these pulses ($R^2 = .18$ – $.24$ and $.32$ – $.40$ in the Oxisol and Mollisol; Figures S8 and S9). Overall, the default MEND model underestimated cumulative C mineralization to a greater extent as anoxic duration increased (Figure 4).

We then employed another parameterization strategy whereby we calibrated the model individually for each treatment to test whether we could discern the key parameters that controlled the decomposition response to O_2 availability. We calibrated two, three, or six parameters that regulate C mineralization processes (see a description of these parameters in Figure S10). We found that the new model could achieve good performance (i.e., lower or comparable AIC, AICc, and/or BIC) with only two free parameters, although the model with six free parameters performed better in CO_2 flux simulations for the Oxisol (Figure S10a–d). Thus, we present the new MEND results from the simulations with two free parameters: the fraction of CH_4 production in total C mineralization (r_{CH_4} , dimensionless) and microbial specific maintenance rate (V_m , $mg\ C\ mg^{-1}\ active-biomass-C\ h^{-1}$) that denotes the microbial maintenance rate per unit active microbial biomass. Overall, model performance in simulating C mineralization data from the fluctuating- O_2 treatments was significantly improved over the previous calibration based on the control treatment only ($R^2 = .46$ – $.73$ and $.60$ – $.73$ in the Oxisol and the Mollisol, respectively; Figures S8e,f, S9 and S10). The AIC values indicated that the new calibrated MEND model outperformed the empirical two-pool first-order statistical model at simulating instantaneous C mineralization rates in the 8- and 12-day treatments, but not in the other treatments (Figures S11 and S12).

In the new calibrated MEND model, we found that r_{CH_4} increased with longer anoxic durations for both soils, although the response was nonlinear for the Oxisol and linear for the Mollisol (Figure S13a,b). The V_m value also linearly ($R^2 = .99$) increased with anoxic duration for the Mollisol (Figure S13d), indicating higher microbial maintenance cost under anoxic than under oxic conditions. However, we did not find any trend in V_m under the fluctuating- O_2 treatments in the Oxisol (Figure S13c).

To synthesize our results from the observations and model simulations, we expressed cumulative C mineralization normalized to the static oxic control as a function of cumulative O_2 availability and the temporal variance in O_2 availability at three representative dates throughout the experiment (days 48, 144, and 384; Figure 4). We found that cumulative C mineralization did not consistently decrease as cumulative O_2 availability declined (Figure 4a,b). In contrast, the MEND model based on traditional assumptions simulated decreasing decomposition with lower O_2 availability due to suppressed microbial activity. For the new calibrated MEND model, the simulations for the Mollisol showed generally similar patterns as the observations, while modeled C mineralization from the Oxisol was still underestimated relative to the observations, although better than under the “old” MEND model.

Temporal O_2 variance ($p < .01$), rather than cumulative O_2 availability ($p < .05$), was a better predictor of cumulative C mineralization at 384 days across both soils. Increased temporal O_2 variance appeared to dampen the effects of increased O_2 availability, resulting in lowest C mineralization in the 2-day treatment, which had the

highest O_2 variance relative to the other fluctuating- O_2 treatments (Figure 4c,d). The MEND model based on traditional assumptions showed a significant influence of O_2 concentration ($p < .01$), but not O_2 variance, on cumulative C mineralization. However, the new calibrated MEND model showed significantly negative effects of increasing O_2 variance on cumulative C mineralization in the Mollisol ($p < .05$), consistent with the observations.

4 | DISCUSSION

In light of our results, we propose a new conceptual view of decomposition responses to temporal variation in O_2 availability to inform theory and mechanistic model development (Figure 1c). We showed that the decomposition rates of slow-cycling C pools decreased as cumulative O_2 availability declined, supporting traditional theory (Freeman et al., 2001; Greenwood, 1961; LaRowe & Van Cappellen, 2011; Lin et al., 2021). However, during our year-long experiment, the fluctuating- O_2 treatments increased either the decomposition rate or size of empirically defined fast-cycling C pools, in contrast to model assumptions (Davidson et al., 2012; Koven et al., 2013; Oleson et al., 2013; Riley et al., 2011; Rubol et al., 2013) and short-term (hours to days) experiments (Bhattacharyya et al., 2018; Sierra et al., 2017). Even in the 12-day treatment, where O_2 was only present 25% of the time, cumulative C decomposition did not differ from the control after weeks–months (Figure 2) because of increased decomposition during oxic periods. The increase in decomposition rates following the anoxic to oxic transition was poorly represented by the initial mechanistic model parameterizations, leading to underestimation of total C loss. Underestimation of CH_4 production in the fluctuating- O_2 treatments with longer anoxic durations also contributed to the model-observation discrepancy. Fluctuating- O_2 treatments with longer anoxic durations lost a greater proportion of C as CH_4 , thereby increasing CO_2 -equivalent greenhouse gas emissions by as much as threefold (Figure 3). Together, these findings demonstrated that oxic/anoxic fluctuations largely sustained, or even transiently stimulated, C decomposition and substantially increased its climate impact on a CO_2 -equivalent basis relative to static oxic conditions over periods of weeks to months.

4.1 | Experiments reveal discrepancies among data, theory, and model assumptions

Our results challenged conventional theory and model assumptions by showing that C decomposition did not monotonically decrease with the cumulative duration of anoxic conditions (Figure 4). Carbon mineralization rate was depressed under the anoxic phases relative to the oxic phases, consistent with traditional theory (Greenwood, 1961). However, intermittent anoxic conditions did not consistently suppress C loss, especially for soil C (Figure S4). The maintenance of high decomposition despite periodic anoxia likely arose from different responses of C availability and molecular C composition to fluctuating- O_2 conditions.

First of all, discrepancies between our observations and the theory/model could be partly ascribed to greater sizes and/or fluxes of the fast-cycling C pool under O_2 fluctuations (Figure 1), linked to changes in C protection mechanisms and bioavailability. Concentrations of DOC increased during anoxic phases (Figure S5), likely due to a combination of kinetic and thermodynamic constraints on anaerobic decomposition (Keiluweit et al., 2017) and the release of mineral-associated C (Buettner et al., 2014; Thompson et al., 2006). In contrast, during the oxic phases DOC declined by as much as $10 \text{ mg C g}^{-1} \text{ C}$ (Figure S5), indicating rapid decomposition corresponding with observed pulses of CO_2 production (Figure 2a,b). The $\delta^{13}C$ measurements of sequential extractions and mineralized C indicated that previously protected soil C released under the anoxic phases provided additional C for microbial decomposition in the presence of O_2 and thus sustained soil C decomposition under

the fluctuating- O_2 treatments (Figures S4 and S6). Replacement of older soil C with litter C in organo-mineral associations (Leinemann et al., 2018) might also have increased the availability and decomposition of soil C under the fluctuating- O_2 treatments (Figure S4). Indeed, significant litter-derived C (~12% of initial litter C on average) ultimately became incorporated in all measured mineral-associated pools (Figure S6). In the Mollisol, the litter was the dominant C source in both the sodium sulfate and sodium pyrophosphate extractions. Release and decomposition of extant mineral-associated C due to disruption of cation bridges by acidification (Ye et al., 2018), as evidenced by carbonate loss in the Mollisol, or following Fe reduction, as observed in both soils (Figure S5), therefore likely contributed to increases in the size of fast C pools in the fluctuating- O_2 treatments with longer anoxic durations in both soils (Table 1). Overall, increased C availability compensated for any depression in C mineralization

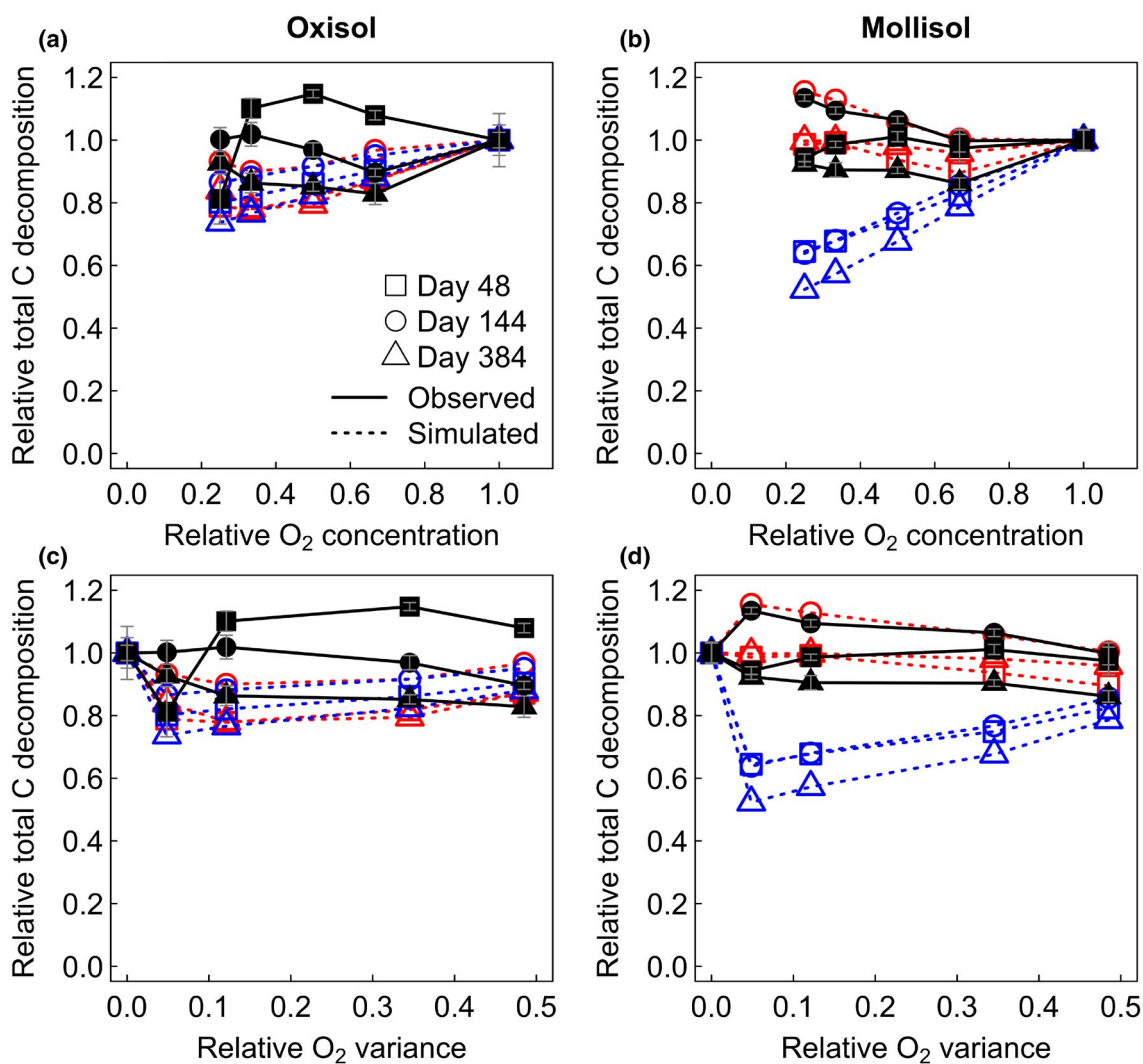


FIGURE 4 Relationships of cumulative C decomposition, normalized to the static oxic controls, with relative O_2 availability (a, b) and temporal variance (c, d) for the Oxisol and Mollisol, respectively. The 2-, 4-, 8-, and 12-day treatments indicate the fluctuating- O_2 treatments, which consisted of repeated cycles of 2, 4, 8, or 12 days of anoxia followed by 4 days of oxic conditions, respectively. The solid lines with closed symbols represent the observations, and the blue and red dotted lines with open symbols represent the simulations by MEND model calibrated with the control only and full dataset, respectively. The error bars indicate SEM ($n = 5$)

due to anoxia after approximately 1 week to 2 months, depending on the particular fluctuating- O_2 treatments and soils (Figure 2).

Moreover, the absence of changes in C chemical composition indicated by ^{13}C NMR (Table S1) further indicated the resilience of long-term decomposition processes to O_2 variability. This contrasts with previous findings of selective protection for reduced C compounds (e.g., lipids and/or lignin) under anoxia (Keiluweit et al., 2017; LaRowe & Van Cappellen, 2011) and the observation of preferential persistence of lignin C under a year-long static anoxic incubation of these same soils (Huang et al., 2020). This latter observation indicates that ^{13}C NMR was sensitive enough to detect meaningful changes in soil C molecular composition if they had occurred. Rather, the absence of change in C composition suggests that microbial taxa able to tolerate periods of anoxia and increase activity during oxic periods (DeAngelis et al., 2010; Pett-Ridge & Firestone, 2005) may have maintained the overall decomposition of molecules with low nominal oxidation state (lipids) and hydrolysis-resistant bonds (lignin). In addition, production of reactive oxygen species during the anoxic/oxic transition, when Fe(II) co-occurred with O_2 , provides another plausible mechanism contributing to decomposition of lignin and lipids despite O_2 deprivation (Chen et al., 2020; Hall et al., 2015; Huang et al., 2019).

4.2 | Modeling C decomposition under fluctuating- O_2 conditions

Calibrating the MEND model with data from all treatments versus the control only showed that results were improved by changing the assumptions of microbial physiology under fluctuating- O_2 conditions. Most ecosystem models that include a mechanistic representation of soil O_2 dynamics assume a consistent decline in decomposition as O_2 decreases, although the precise shape of the response varies among models (Davidson et al., 2012; Koven et al., 2013; Oleson et al., 2013; Riley et al., 2011; Rubol et al., 2013). For this reason, C losses are predicted to be smaller under longer anoxic periods versus shorter ones (Knapp et al., 2008; Waring & Powers, 2016), as simulated by our initial calibration of the MEND model—a result that would also be obtained by other cutting-edge models employing similar assumptions. However, simulations from the MEND model after separate calibration for each treatment suggested that periodic O_2 deprivation did not consistently suppress the decomposition of all C pools (i.e., POM1, POM2, and MAOM; Figure S14).

We used two different modeling approaches, each with different strengths and weaknesses, to understand impacts of O_2 variation on soil C cycling. The two-pool, first-order statistical model fit the data well and demonstrated clear, cumulative impacts of O_2 variation on mathematically defined fast- and slow-cycling C pools over multiple experimental redox cycles (Figure S7). However, such models by definition are incapable of reproducing the observed high-frequency oscillations in C mineralization following anoxic-oxic transitions (Figure S12), and the fitted parameters could not

necessarily be easily extrapolated to other ecosystem contexts. In contrast, the process-based MEND model reproduced the temporal oscillations in C mineralization (Figure S12) but required a more complex structure. Process-based models like MEND inevitably contain many parameters, but as commonly practiced in environmental modeling, most of these are specified a priori based on literature values, and only a limited number of parameters remain to be calibrated in a given study (Luo & Schuur, 2020; Wang et al., 2019; Zhang et al., 2020). In this regard, the information criteria (e.g., AIC) calculated here accounted for the number of free (i.e., calibrated) parameters, not all the parameters (Johnson & Omland, 2004; Zhang et al., 2020). Comparison of AIC values showed that the new calibrated MEND model had better performance (lower AIC, Figure S11) in simulating instantaneous total C mineralization than the first-order two-pool model only under the treatments with longer anoxic durations (i.e., the 8- and 12-day treatments). Better performance of the first-order model than the new calibrated MEND model under the 2- and 4-day treatments may be explained by the small temporal fluctuation in the total C mineralization (Figure S12c–f). The poorer fitting of the flux rates by the MEND model in these treatments was likely due to overestimation of temporal oscillation in C fluxes. This points to the potential issue that the current MEND model may overreact to high temporal variability in O_2 concentrations. However, due to its simple structure, the first-order model by definition could not reproduce the highly fluctuating C mineralization rates observed under longer anoxic durations (Figure S12g–j). Such models cannot inform field-scale modeling with irregular fluctuations in environmental factors such as temperature, moisture, and O_2 .

In general, process-based models differ in scope of application and philosophy relative to simple statistical models where all information to obtain parameters comes from the data alone. The parameterization of the MEND model takes a large amount of information from the literature through the default parameterization of the model, and then adds extra information from the experimental results. To this end, there is an asymmetry in the amount of information that comes from the experiment versus the information coming from the literature. However, complex process-based models offer advantages in terms of mechanistic representation of physical-chemical-biological processes and their interactions (Luo & Schuur, 2020). In short, although the CH_4 -enabled MEND model did not outperform the simple first-order model in simulating C mineralization under short anoxic duration, its mechanistic detail enabled us to test which biogeochemical processes may impact C cycling processes under O_2 fluctuations, paving the way for real-world application beyond the laboratory. Even though the two-pool, first-order model clearly indicated that O_2 fluctuations changed the sizes and decomposition rates of statistically defined C pools, it could not provide insights into underlying mechanisms.

The relative increase in microbial maintenance rate with anoxic duration indicated by the MEND model of the Mollisol (Figure S13) provides a potential mechanistic explanation contributing to

sustained C mineralization under periodic anoxia. Higher microbial maintenance respiration under anoxic conditions is consistent with our first principles understanding that anaerobic metabolisms (respiration, fermentation) yield less energy from per C atom oxidized than aerobic respiration (Pirt, 1965). Accordingly, as microbes allocate more C to sustain their maintenance needs, more C is lost as CO_2 and CH_4 and less C is retained in growing biomass. Because microbial biomass and necromass production are key mechanisms of soil C persistence (Kallenbach et al., 2016), increased maintenance may be an important and largely overlooked mechanism of sustaining C losses in spite of the constraints of O_2 limitation on decomposition. However, we found no consistent relationship between the modeled microbial maintenance parameter and anoxic duration in the Oxisol. This finding may have resulted from an overall lower performance of the model for the Oxisol than the Mollisol, reflecting additional missing processes (such as explicit representation of Fe–C interactions that can protect and decompose C; Chen et al., 2020) that may have obscured a clear response of maintenance respiration to anoxic duration.

Moreover, allowing the ratio of CH_4 production to total C mineralization (r_{CH_4}) to vary with anoxic duration also greatly improved MEND model performance. The default MEND model used a constant baseline r_{CH_4} (0.2), which significantly underestimated CH_4 production (and consequently, CO_2 -equivalent greenhouse gas emissions) under fluctuating- O_2 conditions. The fraction of anaerobic C mineralization released as CH_4 was as great as 0.35 in soils that were exposed to O_2 25% of the time (i.e., for four out of every 16 days; Figure S13), implying the persistence of anaerobic microsites despite periodic O_2 incursions (Angle et al., 2017; Huang & Hall, 2018; Silver et al., 1999). Together, our results point to the importance of accounting for impacts of anoxic conditions on key metrics of microbial physiology to interpret and model impacts of O_2 variability on soil C cycling processes.

Our data-model comparison also indicates a potential role for temporal O_2 variance, beyond cumulative O_2 availability, as a control on C mineralization (Figure 4). Previous work demonstrated that temporal variance in environmental predictors (e.g., temperature) has a differing impact on mean soil respiration that depends on the convex versus concave shape of the response functions: for convex functions, greater predictor variance leads to greater mean soil respiration, whereas for concave functions, greater predictor variance leads to lower mean soil respiration, even when mean predictor values are the same (Sierra et al., 2011). Many models have represented C mineralization as empirical concave-down functions of O_2 concentration (Davidson et al., 2012; Rubol et al., 2013). Although we applied binary anoxic and oxic phases to soils by flushing with nitrogen or air, respectively, in reality these soil samples experienced more gradual changes in O_2 concentrations due to lagged diffusion of O_2 into soil microsites at the beginning of oxic phases (evidenced by persistent CH_4 production; Figure 2), and possibly delayed consumption of microsite O_2 at the beginning of anoxic phases. Therefore, the response of microbial respiration to these continuous spatial and temporal gradients in O_2 availability

might follow a concave, rather than binary, relationship. In this case, we would expect C mineralization to decrease with increasing O_2 variance; this prediction was consistent with our experimental data, where cumulative C decomposition decreased with increased O_2 variance from the 12- to 2-day treatments. Intriguingly, the initial calibration of the MEND model did not predict any relationship between O_2 variance and C mineralization, whereas the new calibrated MEND model did display such a relationship for the Mollisol (Figure 4), despite the fact that it did not explicitly specify a concave or convex relationship between O_2 and C mineralization (this was treated as a binary variable). This suggests that the two key calibrated parameters in the MEND model might be mechanistically related to the hypothesized concave response function of C mineralization to O_2 availability.

5 | CONCLUSION

The occurrence of shifts between anoxic and oxic conditions due to hydrological change is likely to become more frequent in many ecosystems with significant soil C stocks (e.g., croplands in humid biomes (Griffis et al., 2017), ephemeral wetlands (Knapp et al., 2008), arctic permafrost and boreal peatlands (Avis et al., 2011), and wet tropical ecosystems (O'Connell et al., 2018)), where relatively small changes in soil C storage linked to O_2 dynamics could have substantial impacts on climate change (Knoblauch et al., 2018; Schädel et al., 2016). The frequency and magnitude of O_2 fluctuations impact the rate and form (CO_2 vs. CH_4) of C released from these soils and thus impact the C-climate feedback. We showed that traditional model assumptions may substantially underestimate both C loss and CO_2 -equivalent greenhouse gas emissions, driven by high CO_2 and CH_4 production that is sustained under frequent anoxic–oxic transitions over timescales of weeks–months. The results suggest that impacts of O_2 limitation on greenhouse gas emissions depend strongly on the length and temporal variance of the anoxic phase over timescales of days, a factor that is highly sensitive to interactions among physical (e.g., precipitation) and biological processes (e.g., respiration) and is not mechanistically incorporated in current C models. These findings underscore the need to improve a versatile model framework that accounts for the positive and negative impacts of O_2 limitation on C availability to microbes (e.g., organo-mineral interactions), dynamic microbial physiology under O_2 variability (e.g., decomposition resilience and sustained CH_4 production), and co-occurrence of aerobic and anaerobic metabolisms with dynamic microbial physiology that responds to the length of anoxic duration (e.g., microbial maintenance). Our model-data synthesis suggests that simple functions relating O_2 exposure to C mineralization will not necessarily capture the emergent properties of O_2 fluctuations. These attributes will be critical for accurate prediction of changes in the relative and absolute emissions of CO_2 and CH_4 in landscapes with heterogeneous O_2 availability, which have large implications for global greenhouse balances and future biosphere-climate feedbacks.

ACKNOWLEDGMENTS

This research was supported in part by NSF DEB-1457805, EAR-1331841, the Excellent Young Scientists Fund and the National Natural Science Foundation of China (Grant No. 41901059). We thank an anonymous reviewer for helpful comments about temporal O₂ variance and model comparison, Anthony Mirabito and Lucio Reyes for laboratory assistance, and Dr. Jien Zhang for assistance with the hydric soil map.

CONFLICT OF INTEREST

The authors declare no competing interests.

DATA AVAILABILITY STATEMENT

All data needed to evaluate the conclusions in the paper are present in the paper and/or the Supplementary Materials. The incubation data are available from the Environmental Data Initiative Digital Repository (doi: <https://doi.org/10.6073/pasta/1a449825e06e395513f95bdbc891e52a>). Correspondence and requests for materials should be addressed to S.J.H. (stevenjh@iastate.edu) and G.W. (wang.gangsheng@gmail.com).

ORCID

Wenjuan Huang  <https://orcid.org/0000-0003-1038-1591>

Kefeng Wang  <https://orcid.org/0000-0002-8005-269X>

Chenglong Ye  <https://orcid.org/0000-0002-7157-5034>

William C. Hockaday  <https://orcid.org/0000-0002-0501-0393>

Gangsheng Wang  <https://orcid.org/0000-0002-8117-5034>

Steven J. Hall  <https://orcid.org/0000-0002-7841-2019>

REFERENCES

- Angle, J. C., Morin, T. H., Solden, L. M., Narrowe, A. B., Smith, G. J., Borton, M. A., Rey-Sanchez, C., Daly, R. A., Mirfenderesgi, G., Hoyt, D. W., Riley, W. J., Miller, C. S., Bohrer, G., & Wrighton, K. C. (2017). Methanogenesis in oxygenated soils is a substantial fraction of wetland methane emissions. *Nature Communications*, 8(1), 1–9. <https://doi.org/10.1038/s41467-017-01753-4>
- Arndt, S., Jørgensen, B. B., LaRowe, D. E., Middelburg, J. J., Pancost, R. D., & Regnier, P. (2013). Quantifying the degradation of organic matter in marine sediments: A review and synthesis. *Earth-Science Reviews*, 123, 53–86. <https://doi.org/10.1016/j.earscirev.2013.02.008>
- Avis, C. A., Weaver, A. J., & Meissner, K. J. (2011). Reduction in areal extent of high-latitude wetlands in response to permafrost thaw. *Nature Geoscience*, 4(7), 444–448. <https://doi.org/10.1038/ngeo1160>
- Bates, D., Mächler, M., Bolker, B., & Walker, S. (2015). Fitting linear mixed-effects models using lme4. *Journal of Statistical Software*, 67(1), 1–48.
- Bhattacharyya, A., Campbell, A. N., Tfaily, M. M., Lin, Y., Kukkadapu, R. K., Silver, W. L., Nico, P. S., & Pett-Ridge, J. (2018). Redox fluctuations control the coupled cycling of iron and carbon in tropical forest soils. *Environmental Science & Technology*, 52(24), 14129–14139. <https://doi.org/10.1021/acs.est.8b03408>
- Bradford, M. A., Wieder, W. R., Bonan, G. B., Fierer, N., Raymond, P. A., & Crowther, T. W. (2016). Managing uncertainty in soil carbon feedbacks to climate change. *Nature Climate Change*, 6(8), 751–758. <https://doi.org/10.1038/nclimate3071>
- Buettner, S. W., Kramer, M. G., Chadwick, O. A., & Thompson, A. (2014). Mobilization of colloidal carbon during iron reduction in basaltic soils. *Geoderma*, 221–222, 139–145. <https://doi.org/10.1016/j.geoderma.2014.01.012>
- Burdige, D. J. (2007). Preservation of organic matter in marine sediments: Controls, mechanisms, and an imbalance in sediment organic carbon budgets? *Chemical Reviews*, 107(2), 467–485. <https://doi.org/10.1021/cr050347q>
- Buss, H. L., Chapela Lara, M., Moore, O. W., Kurtz, A. C., Schulz, M. S., & White, A. F. (2017). Lithological influences on contemporary and long-term regolith weathering at the Luquillo Critical Zone Observatory. *Geochimica et Cosmochimica Acta*, 196, 224–251. <https://doi.org/10.1016/j.gca.2016.09.038>
- Calabrese, S., & Porporato, A. (2019). Impact of ecohydrological fluctuations on iron-redox cycling. *Soil Biology and Biochemistry*, 133, 188–195. <https://doi.org/10.1016/j.soilbio.2019.03.013>
- Chacon, N., Silver, W. L., Dubinsky, E. A., & Cusack, D. F. (2006). Iron reduction and soil phosphorus solubilization in humid tropical forests soils: The roles of labile carbon pools and an electron shuttle compound. *Biogeochemistry*, 78(1), 67–84. <https://doi.org/10.1007/s10533-005-2343-3>
- Chen, C., Hall, S. J., Coward, E., & Thompson, A. (2020). Iron-mediated organic matter decomposition in humid soils can counteract protection. *Nature Communications*, 11(1), 1–13. <https://doi.org/10.1038/s41467-020-16071-5>
- Chen, C., Meile, C., Wilmoth, J., Barcellos, D., & Thompson, A. (2018). Influence of pO₂ on iron redox cycling and anaerobic organic carbon mineralization in a humid tropical forest soil. *Environmental Science & Technology*, 52(14), 7709–7719. <https://doi.org/10.1021/acs.est.8b01368>
- Conrad, R. (1996). Soil microorganisms as controllers of atmospheric trace gases (H₂, CO, CH₄, OCS, N₂O, and NO). *Microbiological Reviews*, 60(4), 609–640. <https://doi.org/10.1128/mr.60.4.609-640.1996>
- Coward, E. K., Thompson, A. T., & Plante, A. F. (2017). Iron-mediated mineralogical control of organic matter accumulation in tropical soils. *Geoderma*, 306, 206–216. <https://doi.org/10.1016/j.geoderma.2017.07.026>
- Davidson, E. A., Samanta, S., Caramori, S. S., & Savage, K. (2012). The Dual Arrhenius and Michaelis-Menten kinetics model for decomposition of soil organic matter at hourly to seasonal time scales. *Global Change Biology*, 18(1), 371–384. <https://doi.org/10.1111/j.1365-2486.2011.02546.x>
- DeAngelis, K. M., Silver, W. L., Thompson, A. W., & Firestone, M. K. (2010). Microbial communities acclimate to recurring changes in soil redox potential status. *Environmental Microbiology*, 12(12), 3137–3149. <https://doi.org/10.1111/j.1462-2920.2010.02286.x>
- Duan, Q., Sorooshian, S., & Gupta, V. (1992). Effective and efficient global optimization for conceptual rainfall-runoff models. *Water Resources Research*, 28(4), 1015–1031. <https://doi.org/10.1029/91WR02985>
- Freeman, C., Ostle, N., & Kang, H. (2001). An enzymic “latch” on a global carbon store. *Nature*, 409, 149. <https://doi.org/10.1038/35051650>
- Greenwood, D. J. (1961). The effect of oxygen concentration on the decomposition of organic materials in soil. *Plant and Soil*, 14(4), 360–376. <https://doi.org/10.1007/BF01666294>
- Griffis, T. J., Chen, Z., Baker, J. M., Wood, J. D., Millet, D. B., Lee, X., Venterea, R. T., & Turner, P. A. (2017). Nitrous oxide emissions are enhanced in a warmer and wetter world. *Proceedings of the National Academy of Sciences of the United States of America*, 114(45), 12081–12085. <https://doi.org/10.1073/pnas.1704552114>
- Hall, S. J., Huang, W., & Hammel, K. E. (2017). An optical method for carbon dioxide isotopes and mole fractions in small gas samples: Tracing microbial respiration from soil, litter, and lignin. *Rapid Communications in Mass Spectrometry*, 31(22), 1938–1946. <https://doi.org/10.1002/rcm.7973>
- Hall, S. J., McDowell, W. H., & Silver, W. L. (2013). When wet gets wetter: Decoupling of moisture, redox biogeochemistry, and greenhouse gas fluxes in a humid tropical forest soil. *Ecosystems*, 16(4), 576–589. <https://doi.org/10.1007/s10021-012-9631-2>

- Hall, S. J., Silver, W. L., Timokhin, V. I., & Hammel, K. E. (2015). Lignin decomposition is sustained under fluctuating redox conditions in humid tropical forest soils. *Global Change Biology*, 21(7), 2818–2828. <https://doi.org/10.1111/gcb.12908>
- Hatfield, J. L., Jaynes, D. B., Burkart, M. R., Cambardella, C. A., Moorman, T. B., Prueger, J. H., & Smith, M. A. (1999). Water quality in Walnut Creek watershed: Setting and farming practices. *Journal of Environmental Quality*, 28(1), 11–24. <https://doi.org/10.2134/jeq1999.00472425002800010002x>
- Huang, W., & Hall, S. J. (2017a). Optimized high-throughput methods for quantifying iron biogeochemical dynamics in soil. *Geoderma*, 306, 67–72. <https://doi.org/10.1016/j.geoderma.2017.07.013>
- Huang, W., & Hall, S. J. (2017b). Elevated moisture stimulates carbon loss from mineral soils by releasing protected organic matter. *Nature Communications*, 8(1), 1774. <https://doi.org/10.1038/s41467-017-01998-z>
- Huang, W., & Hall, S. J. (2018). Large impacts of small methane fluxes on carbon isotope values of soil respiration. *Soil Biology and Biochemistry*, 124, 126–133. <https://doi.org/10.1016/j.soilbio.2018.06.003>
- Huang, W., Hammel, K. E., Hao, J., Thompson, A., Timokhin, V. I., & Hall, S. J. (2019). Enrichment of lignin-derived carbon in mineral-associated soil organic matter. *Environmental Science & Technology*, 53(13), 7522–7531. <https://doi.org/10.1021/acs.est.9b01834>
- Huang, W., Ye, C., Hockaday, W. C., & Hall, S. J. (2020). Trade-offs in soil carbon protection mechanisms under aerobic and anaerobic conditions. *Global Change Biology*, 26(6), 3726–3737. <https://doi.org/10.1111/gcb.15100>
- IPCC. (2014). *Climate change 2014: Impacts, adaptation, and vulnerability. Part A: Global and sectoral aspects. Contribution of working group II to the fifth assessment report of the Intergovernmental Panel on Climate Change*. In C. B. Field, V. R. Barros, D. J. Dokken, K. J. Mach, M. D. Mastrandrea, T. E. Bilir, M. Chatterjee, K. L. Ebi, Y. O. Estrada, R. C. Genova, B. Girma, E. S. Kissel, A. N. Levy, S. MacCracken, P. R. Mastrandrea, & L. L. White (Eds.). Cambridge University Press.
- Jarecke, K. M., Loecke, T. D., & Burgin, A. J. (2016). Coupled soil oxygen and greenhouse gas dynamics under variable hydrology. *Soil Biology and Biochemistry*, 95, 164–172. <https://doi.org/10.1016/j.soilbio.2015.12.018>
- Jian, S., Li, J., Wang, G., Kluber, L. A., Schadt, C. W., Liang, J., & Mayes, M. A. (2020). Multi-year incubation experiments boost confidence in model projections of long-term soil carbon dynamics. *Nature Communications*, 11(1), 5864. <https://doi.org/10.1038/s41467-020-19428-y>
- Johnson, J. B., & Omland, K. S. (2004). Model selection in ecology and evolution. *Trends in Ecology & Evolution*, 19(2), 101–108. <https://doi.org/10.1016/j.tree.2003.10.013>
- Kallenbach, C. M., Frey, S. D., & Grandy, A. S. (2016). Direct evidence for microbial-derived soil organic matter formation and its ecophysiological controls. *Nature Communications*, 7, 13630. <https://doi.org/10.1038/ncomms13630>
- Keiluweit, M., Nico, P. S., Kleber, M., & Fendorf, S. (2016). Are oxygen limitations under recognized regulators of organic carbon turnover in upland soils? *Biogeochemistry*, 127(2–3), 157–171. <https://doi.org/10.1007/s10533-015-0180-6>
- Keiluweit, M., Wanzek, T., Kleber, M., Nico, P., & Fendorf, S. (2017). Anaerobic microsites have an unaccounted role in soil carbon stabilization. *Nature Communications*, 8(1), 1771. <https://doi.org/10.1038/s41467-017-01406-6>
- Knapp, A. K., Beier, C., Briske, D. D., Classen, A. T., Luo, Y., Reichstein, M., Smith, M. D., Smith, S. D., Bell, J. E., Fay, P. A., Heisler, J. L., Leavitt, S. W., Sherry, R., Smith, B., & Weng, E. (2008). Consequences of more extreme precipitation regimes for terrestrial ecosystems. *BioScience*, 58(9), 811–821. <https://doi.org/10.1641/B580908>
- Knoblauch, C., Beer, C., Liebner, S., Grigoriev, M. N., & Pfeiffer, E.-M. (2018). Methane production as key to the greenhouse gas budget of thawing permafrost. *Nature Climate Change*, 8(4), 309–312. <https://doi.org/10.1038/s41558-018-0095-z>
- Koven, C. D., Riley, W. J., Subin, Z. M., Tang, J. Y., Torn, M. S., Collins, W. D., Bonan, G. B., Lawrence, D. M., & Swenson, S. C. (2013). The effect of vertically resolved soil biogeochemistry and alternate soil C and N models on C dynamics of CLM4. *Biogeosciences*, 10(11), 7109–7131. <https://doi.org/10.5194/bg-10-7109-2013>
- LaRowe, D. E., & Van Cappellen, P. (2011). Degradation of natural organic matter: A thermodynamic analysis. *Geochimica et Cosmochimica Acta*, 75(8), 2030–2042. <https://doi.org/10.1016/j.gca.2011.01.020>
- Leinemann, T., Preusser, S., Mikutta, R., Kalbitz, K., Cerli, C., Höschel, C., Mueller, C. W., Kandeler, E., & Guggenberger, G. (2018). Multiple exchange processes on mineral surfaces control the transport of dissolved organic matter through soil profiles. *Soil Biology and Biochemistry*, 118, 79–90. <https://doi.org/10.1016/j.soilbio.2017.12.006>
- Lin, Y., Campbell, A. N., Bhattacharyya, A., DiDonato, N., Thompson, A. M., Tfaily, M. M., Nico, P. S., Silver, W. L., & Pett-Ridge, J. (2021). Differential effects of redox conditions on the decomposition of litter and soil organic matter. *Biogeochemistry*, 154(1), 1–15. <https://doi.org/10.1007/s10533-021-00790-y>
- Liptzin, D., Silver, W. L., & Detto, M. (2011). Temporal dynamics in soil oxygen and greenhouse gases in two humid tropical forests. *Ecosystems*, 14(2), 171–182. <https://doi.org/10.1007/s10021-010-9402-x>
- Logsdon, S. D. (2015). Event- and site-specific soil wetting and seasonal change in amount of soil water. *Soil Science Society of America Journal*, 79(3), 730–741. <https://doi.org/10.2136/sssaj2014.08.0327>
- Longhi, D., Bartoli, M., Nizzoli, D., Laini, A., & Viaroli, P. (2016). Do oxic-anoxic transitions constrain organic matter mineralization in eutrophic freshwater wetlands? *Hydrobiologia*, 774(1), 81–92. <https://doi.org/10.1007/s10750-016-2722-x>
- Luo, Y., & Schuur, E. A. G. (2020). Model parameterization to represent processes at unresolved scales and changing properties of evolving systems. *Global Change Biology*, 26(3), 1109–1117. <https://doi.org/10.1111/gcb.14939>
- McLatchey, G. P., & Reddy, K. R. (1998). Regulation of organic matter decomposition and nutrient release in a wetland soil. *Journal of Environmental Quality*, 27(5), 1268–1274. <https://doi.org/10.2134/jeq1998.00472425002700050036x>
- Meile, C., & Scheibe, T. D. (2018). Reactive transport modeling and biogeochemical cycling. *Reactive transport modeling* (pp. 485–510). John Wiley & Sons, Ltd. <https://doi.org/10.1002/9781119060031.ch10>
- Myhre, G., Shindell, D., Bréon, F.-M., Collins, W., Fuglestedt, J., Huang, J., Koch, D., Lamarque, J.-F., Lee, D., Mendoza, B., Nakajima, T., Robock, A., Stephens, G., Takemura, T., & Zhang, H. (2013). Anthropogenic and natural radiative forcing. In T. F. Stocker, D. Qin, G.-K. Plattner, M. Tignor, S. K. Allen, J. Doschung, A. Nauels, Y. Xia, V. Bex, & P. M. Midgley (Eds.), *Climate change 2013: The physical science basis. Contribution of working group I to the fifth assessment report of the Intergovernmental Panel on Climate Change* (pp. 659–740). Cambridge University Press. <https://doi.org/10.1017/CBO9781107415324.018>
- O'Connell, C. S., Ruan, L., & Silver, W. L. (2018). Drought drives rapid shifts in tropical rainforest soil biogeochemistry and greenhouse gas emissions. *Nature Communications*, 9(1), 1348. <https://doi.org/10.1038/s41467-018-03352-3>
- Oleson, K. W., Lawrence, D. M., Bonan, G. B., Drewniak, B., Huang, M., Levis, S., Li, F., Riley, W. J., Swenson, S. C., Thornton, P. E., Bozbiyik, A., Fisher, R., Heald, C. L., Kluzek, E., Lamarque, F., Lawrence, P. J., Leung, L. R., Muszala, S., Ricciuto, D. M., ... Yang, Z.-L. (2013). Technical Description of version 4.5 of the Community Land Model (CLM), 434.
- Pett-Ridge, J., & Firestone, M. K. (2005). Redox fluctuation structures microbial communities in a wet tropical soil. *Applied and Environmental Microbiology*, 71(11), 6998–7007. <https://doi.org/10.1128/AEM.71.11.6998-7007.2005>

- Piao, S., Friedlingstein, P., Ciais, P., de Noblet-Ducoudré, N., Labat, D., & Zaehle, S. (2007). Changes in climate and land use have a larger direct impact than rising CO₂ on global river runoff trends. *Proceedings of the National Academy of Sciences of the United States of America*, 104(39), 15242–15247. <https://doi.org/10.1073/pnas.0707213104>
- Pirt, S. J. (1965). The maintenance energy of bacteria in growing cultures. *Proceedings of the Royal Society of London. Series B, Biological Sciences*, 163(991), 224–231. <https://doi.org/10.1098/rspb.1965.0069>
- Reddy, K. R., & Patrick, W. H. (1975). Effect of alternate aerobic and anaerobic conditions on redox potential, organic matter decomposition and nitrogen loss in a flooded soil. *Soil Biology and Biochemistry*, 7(2), 87–94. [https://doi.org/10.1016/0038-0717\(75\)90004-8](https://doi.org/10.1016/0038-0717(75)90004-8)
- Riley, W. J., Subin, Z. M., Lawrence, D. M., Swenson, S. C., Torn, M. S., Meng, L., Mahowald, N. M., & Hess, P. (2011). Barriers to predicting changes in global terrestrial methane fluxes: Analyses using CLM4Me, a methane biogeochemistry model integrated in CESM. *Biogeosciences*, 8(7), 1925–1953. <https://doi.org/10.5194/bg-8-1925-2011>
- Rubol, S., Manzoni, S., Bellin, A., & Porporato, A. (2013). Modeling soil moisture and oxygen effects on soil biogeochemical cycles including dissimilatory nitrate reduction to ammonium (DNRA). *Advances in Water Resources*, 62, 106–124. <https://doi.org/10.1016/j.advwatres.2013.09.016>
- Schädel, C., Bader, M.-F., Schuur, E. A. G., Biasi, C., Bracho, R., Čapek, P., De Baets, S., Diáková, K., Ernakovich, J., Estop-Aragones, C., Graham, D. E., Hartley, I. P., Iversen, C. M., Kane, E., Knoblauch, C., Lupascu, M., Martikainen, P. J., Natali, S. M., Norby, R. J., ... Wickland, K. P. (2016). Potential carbon emissions dominated by carbon dioxide from thawed permafrost soils. *Nature Climate Change*, 6(10), 950–953. <https://doi.org/10.1038/nclimate3054>
- Sierra, C. A., Harmon, M. E., Thomann, E., Perakis, S. S., & Loescher, H. W. (2011). Amplification and dampening of soil respiration by changes in temperature variability. *Biogeosciences*, 8(4), 951–961. <https://doi.org/10.5194/bg-8-951-2011>
- Sierra, C. A., Malghani, S., & Loescher, H. W. (2017). Interactions among temperature, moisture, and oxygen concentrations in controlling decomposition rates in a boreal forest soil. *Biogeosciences*, 14(3), 703–710. <https://doi.org/10.5194/bg-14-703-2017>
- Silver, W. L., Lugo, A. E., & Keller, M. (1999). Soil oxygen availability and biogeochemistry along rainfall and topographic gradients in upland wet tropical forest soils. *Biogeochemistry*, 44(3), 301–328. <https://doi.org/10.1023/A:1006034126698>
- Soil Survey Staff, Natural Resources Conservation Service, United States Department of Agriculture. (2019). Web soil survey. <https://websoilsurvey.nrcs.usda.gov/>
- Thompson, A., Chadwick, O. A., Boman, S., & Chorover, J. (2006). Colloid mobilization during soil iron redox oscillations. *Environmental Science & Technology*, 40(18), 5743–5749. <https://doi.org/10.1021/es061203b>
- Wagai, R., & Mayer, L. M. (2007). Sorptive stabilization of organic matter in soils by hydrous iron oxides. *Geochimica et Cosmochimica Acta*, 71(1), 25–35. <https://doi.org/10.1016/j.gca.2006.08.047>
- Wang, G., Huang, W., Mayes, M. A., Liu, X., Zhang, D., Zhang, Q., Han, T., & Zhou, G. (2019). Soil moisture drives microbial controls on carbon decomposition in two subtropical forests. *Soil Biology and Biochemistry*, 130, 185–194. <https://doi.org/10.1016/j.soilbio.2018.12.017>
- Wang, G., Jagadamma, S., Mayes, M. A., Schadt, C. W., Megan Steinweg, J., Gu, L., & Post, W. M. (2015). Microbial dormancy improves development and experimental validation of ecosystem model. *The ISME Journal*, 9(1), 226–237. <https://doi.org/10.1038/ismej.2014.120>
- Wang, G., & Post, W. M. (2012). A theoretical reassessment of microbial maintenance and implications for microbial ecology modeling. *FEMS Microbiology Ecology*, 81(3), 610–617. <https://doi.org/10.1111/j.1574-6941.2012.01389.x>
- Wang, G., Post, W. M., & Mayes, M. A. (2013). Development of microbial-enzyme-mediated decomposition model parameters through steady-state and dynamic analyses. *Ecological Applications*, 23(1), 255–272. <https://doi.org/10.1890/12-0681.1>
- Waring, B. G., & Powers, J. S. (2016). Unraveling the mechanisms underlying pulse dynamics of soil respiration in tropical dry forests. *Environmental Research Letters*, 11(10), 105005. <https://doi.org/10.1088/1748-9326/11/10/105005>
- Whiticar, M. J. (1999). Carbon and hydrogen isotope systematics of bacterial formation and oxidation of methane. *Chemical Geology*, 161, 291–314. [https://doi.org/10.1016/s0009-2541\(99\)00092-3](https://doi.org/10.1016/s0009-2541(99)00092-3)
- Ye, C., Chen, D., Hall, S. J., Pan, S., Yan, X., Bai, T., Guo, H., Zhang, Y., Bai, Y., & Hu, S. (2018). Reconciling multiple impacts of nitrogen enrichment on soil carbon: Plant, microbial and geochemical controls. *Ecology Letters*, 21(8), 1162–1173. <https://doi.org/10.1111/ele.13083>
- Zhang, H., Goll, D. S., Wang, Y.-P., Ciais, P., Wieder, W. R., Abramoff, R., Huang, Y., Guenet, B., Prescher, A.-K., Rossel, R. A. V., Barré, P., Chenu, C., Zhou, G., & Tang, X. (2020). Microbial dynamics and soil physicochemical properties explain large-scale variations in soil organic carbon. *Global Change Biology*, 26(4), 2668–2685. <https://doi.org/10.1111/gcb.14994>
- Zhu, Q., Liu, J., Peng, C., Chen, H., Fang, X., Jiang, H., Yang, G., Zhu, D., Wang, W., & Zhou, X. (2014). Modelling methane emissions from natural wetlands by development and application of the TRIPLEX-GHG model. *Geoscientific Model Development*, 7(3), 981–999. <https://doi.org/10.5194/gmd-7-981-2014>

SUPPORTING INFORMATION

Additional Supporting Information may be found online in the Supporting Information section.

How to cite this article: Huang, W., Wang, K., Ye, C., Hockaday, W. C., Wang, G., & Hall, S. J. (2021). High carbon losses from oxygen-limited soils challenge biogeochemical theory and model assumptions. *Global Change Biology*, 27, 6166–6180. <https://doi.org/10.1111/gcb.15867>